ISSN 1995-0780, Nanotechnologies in Russia, 2016, Vol. 11, Nos. 5–6, pp. 280–286. © Pleiades Publishing, Ltd., 2016.
Original Russian Text © S.V. Zaitsev, V.M. Nartsev, V.S. Vashchilin, D.S. Prokhorenkov, E.I. Evtushenko, 2016, published in Rossiiskie Nanotekhnologii, 2016, Vol. 11, Nos. 5–6.

Microstructure and Surface Morphology of Thin AlN Films Formed on Sapphire by Dual Magnetron Sputtering

S. V. Zaitsev, V. M. Nartsev, V. S. Vashchilin, D. S. Prokhorenkov, and E. I. Evtushenko

Shukhov Belgorod State Technological University, ul. Kostyukova 46, Belgorod, 308012 Russia

e-mail: eveviv@intbel.ru

Received June 19, 2015; in final form, February 15, 2016

Abstract—Results of studies of the effect of the discharge current on the crystalline structure, surface morphology, and thickness of thin AlN coatings deposited by reactive dual magnetron sputtering on *c*-axis oriented sapphire wafers have been described. Using grazing incidence X-ray diffraction, it has been determined that the coatings have a wurtzite crystalline structure and at least two types of grains with different orientations of the (002) planes. Electron microscopy has revealed that the coatings are composed of vertically aligned columnar grains and a nucleation layer. The grains are uniformly distributed over the substrate surface; each of the grains consists of smaller crystallites. It has been found that the discharge current largely affects the concentration of grains of different orientations and has hardly any effect on the size of the nuclei.

DOI: 10.1134/S1995078016030186

INTRODUCTION

The physicochemical properties of aluminum nitride (AlN) make it a promising material for a variety of semiconductor devices. The bandgap of 6.2 eV provides the use of AlN as a material for optoelectronic devices operating in the violet and ultraviolet spectral regions [1–3]. This compound exhibits a low dielectric loss and thermal expansion coefficient; therefore, it can be used for designing electronic equipment components that reliably operate even under extreme conditions. In addition, owing to the high adhesion strength of aluminum nitride, it is used as protective and impact-resistant coatings [4–6]. Today, the most interesting trend is the establishment of high-performance nitride-based microelectronics, which requires the development of a technology for the deposition of AlN coatings with a controlled morphology and a high quality of the crystalline structure. In particular, single-crystal AlN layers with a low defect content are required.

At present, there are many methods for forming thin AlN coatings, such as chemical vapor deposition, pulsed laser deposition, molecular beam epitaxy, and magnetron sputtering [7–10]. Reactive magnetron sputtering makes it possible to prepare coatings at low temperatures; conduct a layer-by-layer synthesis of novel structures; and, above all, control the morphology of the layers over a wide range [11–14]. In the magnetron method, the coating structure is technologically controlled through the operating pressure; the reaction gas fraction; and the discharge current, voltage, and frequency [15]. The aim of this study is to examine the effect of magnetron discharge current on

Table 1. Aluminum nitride deposition conditions

Parameters	Description
Targets	Al (99.999% purity, 372 × 74 × 6 mm), two vertically mounted pieces
Working gas	Ar (99.999% special purity grade)
Reaction gas	N_2 (99.999% special purity grade)
Volume fraction of N_2, %	30
Magnetron discharge current, A	6, 7, 8, 9
Voltage, V	334–405
Frequency, kHz	20
Rotation of a roundabout with samples, rpm	18

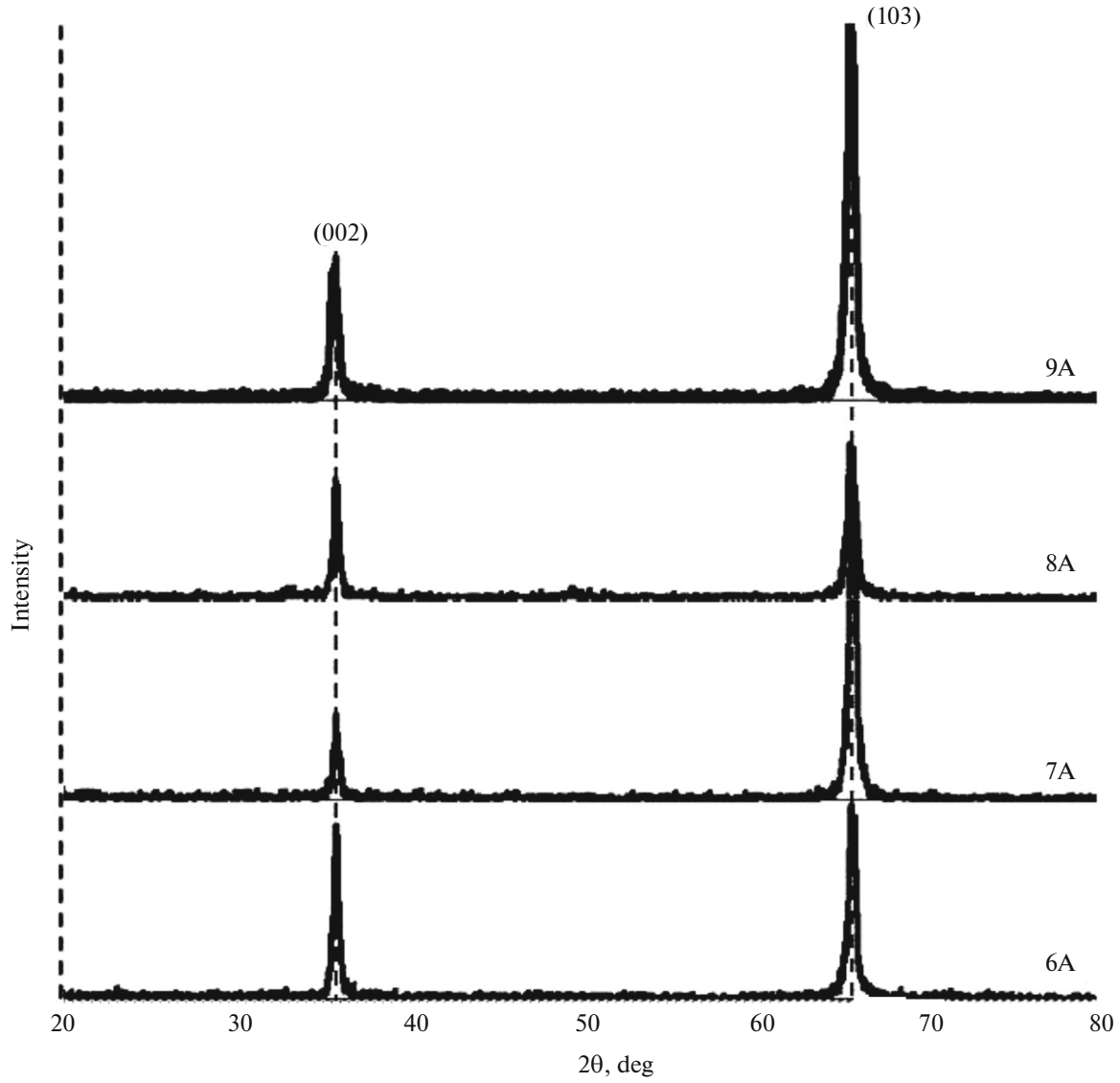

Fig. 1. X-ray diffraction patterns of the AlN coatings deposited at different discharge currents.

the morphology and microstructure of aluminum nitride coatings.

MATERIALS AND METHODS

Aluminum nitride was deposited by dual magnetron sputtering using a QUADRA 500TM vacuum setup. *c*-axis oriented sapphire substrates were placed on the object stage in the vacuum chamber. Before coating deposition, the substrates were subjected to ultrasonic cleaning in acetone and ethanol, washed in deionized water, and then dried with pure nitrogen. The vacuum chamber was evacuated to a pressure below 5×10^{-3} Pa using a turbomolecular pump. Working gases (Ar and N_2) were fed into the chamber separately and controlled using mass flow controllers. The distance from the substrate to the magnetron and the ion sources was the same—70 mm. The coating was deposited for 120 min after a preliminary 10-min ion-beam cleaning of the substrates. The working gas pressure in the chamber was 0.22 Pa. Table 1 shows the aluminum nitride deposition conditions.

The crystalline structure of thin AlN films was studied by X-ray diffraction (ARL X'TRA, Thermo-Techno) in an asymmetric coplanar recording mode at a grazing incidence angle of $\alpha = 3°$ (θ-scan) to exclude substrate peaks. Phase identification and peak index-

Table 2. Characteristics of the diffraction reflections of surfaces at different discharge currents

Discharge current, A	Diffraction angle (2θ scale), deg	Plane	Full width at half maximum (2θ scale), deg	Intensity, pps	$I_{(103)}/(I_{(002)} + I_{(103)})$	L_{CSR}, nm
6	35.660	(002)	0.620	387	0.58	13.1
	65.680	(103)	0.735	525		12.6
7	35.700	(002)	0.650	166	0.83	12.5
	65.700	(103)	0.740	833		12.5
8	35.700	(002)	0.645	284	0.59	12.6
	65.640	(103)	0.830	403		11.1
9	35.600	(002)	0.725	365	0.75	11.2
	65.600	(103)	0.790	1082		11.7

ation were conducted according to the JCPDF database.

The $\gamma_{(002)}$ and $\gamma_{(103)}$ angles between the *c* axis of the AlN coating and the normal to the sample surface, i.e., the *c* axis of the sapphire substrate, were determined according to peaks of the respective planes from the recording geometry using the formulas

$$\gamma_{(002)} = \theta_{(002)} - \alpha, \quad \gamma_{(103)} = \Delta - \theta_{(103)} - \alpha, \quad (1)$$

where $\theta_{(002)}$ and $\theta_{(103)}$ are the diffraction angles at which the respective planes are observed and Δ is the angle between the (002) and (103) planes for AlN (according to measurements, $\Delta \approx 32.08^\circ$).

For all the peaks, sizes of X-ray coherent scattering regions L_{CSR}, i.e., nucleation centers, were calculated by the Scherrer formula

$$L_{CSR} = \frac{k\lambda}{\beta\cos\theta}, \quad (2)$$

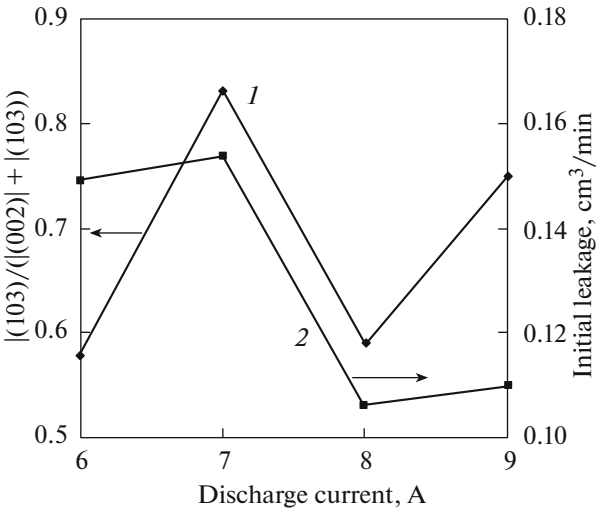

Fig. 2. Dependences of (*1*) the relative fraction of grains with the (002) orientation and (*2*) the initial leakage on discharge current.

where $k = 0.878$ is the averaged constant calculated from the model X-ray diffraction pattern of finite-size AlN grains for the (002) and (103) peaks, $\lambda = 0.1541744$ nm is the X-ray wavelength, β is the full width at half maximum of the reflection in radians (2θ scale), and θ is the angle at which the diffraction peak is observed [16]. In calculations according to Eq. (2), the contributions of grain stresses to the peak width were ignored.

Diameter *d* and height *h* of the nuclei were determined using the following formulas:

$$d = L_{CSR}/\sin(\theta), \quad (3)$$

$$h = d \cdot \tan(\alpha). \quad (4)$$

The morphology of surfaces and cleavages of the coatings was studied using a Tescan MIRA3 LMU scanning electron microscope.

RESULTS AND DISCUSSION

According to X-ray diffraction, all the synthesized coatings have an AlN crystalline structure (Fig. 1).

The presence only of reflections of the (002) and (103) planes indicates the orientation of the crystalline structure of the coatings. In the θ-scan recording mode, the presence of a (103) peak suggests that the coating contains grains whose *c* axis deviates from the normal to the substrate plane by an angle of ~2.3°. The (002) peak indicates the presence of grains whose *c* axis deviates from the normal to the substrate plane by ~14.3°. Note that similar relationships were recorded in [17]. The most probable causes of the formation of grains with different orientations of the (002) planes are a mismatch between the *c* plane of α-Al_2O_3 and the crystallographic planes of AlN, a high energy of the Al–N bond responsible for the low mobility of the deposited Al and N atoms on the growing surface, and a large-scale nucleation caused by a large flow of atoms deposited on the substrate.

Table 2 shows characteristics of the diffraction peaks, ratios of their intensities, and data on L_{CSR}. The $I_{(103)}/(I_{(002)} + I_{(103)})$ values for the (103) and (002)

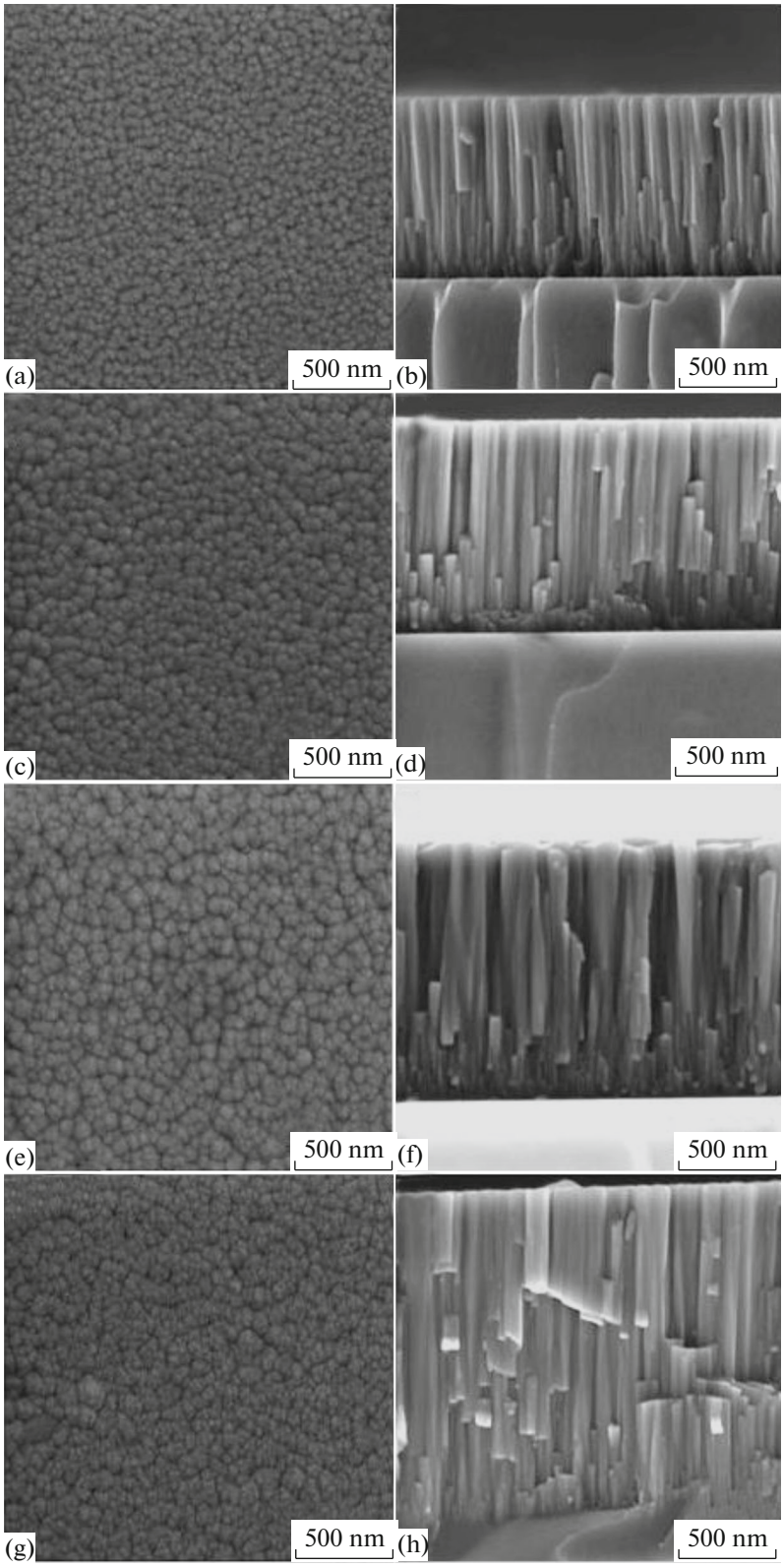

Fig. 3. (a, c, e, g) Surface morphology and (b, d, f, h) fracture patterns of the AlN coatings prepared at different discharge currents: (a, b) 6 A; (c, d) 7 A; (e, f) 8 A; and (g, h) 9 A.

Table 3. Characteristics of the coatings

Current, A	Coating thickness, nm	Average grain size, nm
6	1166	54
7	1493	73
8	1872	74
9	2268	81

peaks suggest that the coating deposited at 7 A has a maximum relative concentration of grains whose crystallographic *c* axes are nearly perpendicular to the substrate plane. The similarity of the dependences of the fraction of grains with the (002) orientation and the initial leakage in the sputtering chamber (Fig. 2) indicates a significant effect of impurities on the nucleation of the crystalline structure of the coating. Apparently, the increased flow of impurities at the beginning of the process effectively inhibits the growth of the grains whose *c* axes significantly deviate from the *c* axis of the sapphire substrate. This effect can be used to modify magnetron sputtering for controlling the orientation of aluminum nitride grains on sapphire. It should be noted that the dependences shown in Fig. 2 are given for descriptive reasons, because the initial leakage, i.e., the initial flow of impurities, does not depend on the discharge current. However, the growth of grains of different orientations depends on the discharge current, which determines the intensity of the flow of N and Al atoms onto the substrate.

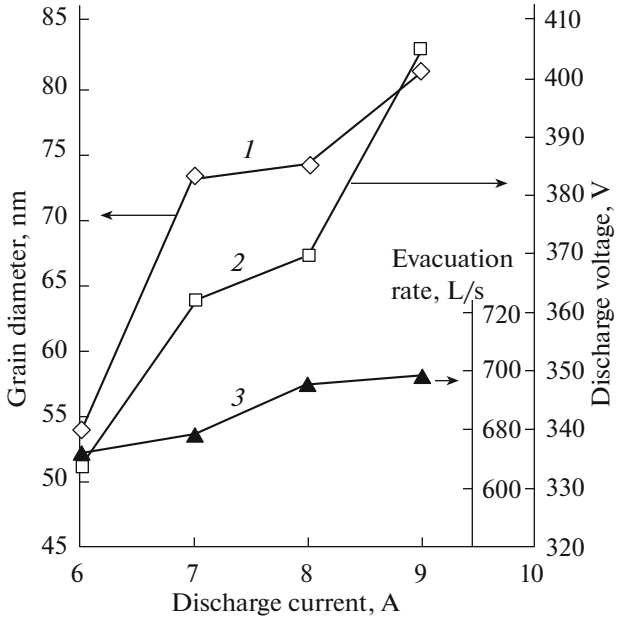

Fig. 4. Dependences of (*1*) average grain diameter, (*2*) discharge voltage, and (*3*) evacuation rate on discharge current.

Calculations from L_{CSR} values with allowance for the AlN structure show that, in this recording configuration, the samples contain large and small nuclei. The small nuclei have a diameter of ~22.1 nm and a height of ~1.2 nm; their *c* axis is nearly perpendicular to the substrate plane. The large nuclei presumably have a diameter of ~40.3 nm, a height of ~2.1 nm, and an angle of ~14.3° between the *c* axis and the normal to the substrate, which corresponds to the intergrowth of the (002) plane of the sapphire and the (107) plane of the aluminum nitride.

Figure 3 shows the surface morphology and fracture patterns of the thin AlN coatings on sapphire.

According to Figs. 3a, 3c, 3e, and 3g, the grains are uniformly distributed over the substrate surface; each grain consists of smaller crystallites; this fact indicates the formation of unhealable defects (presumably, threadlike dislocations and low-angle boundaries). The fracture patterns (Figs. 3b, 3d, 3f, 3h) show that the coatings consist of vertically aligned columnar grains and a nucleation layer. In this layer, at least two types of nuclei can be detected for each sample; the diameters and orientations of the *c* axes of these nuclei are close to the X-ray diffraction data. The average grain sizes and coating thicknesses determined by microscopy are listed in Table 3.

An increase in the average grain size with an increasing current strength can be attributed to an increase in the coating thickness. Thus, in the case of deposition of thick coatings, there is a higher statistical probability of the growth of large grains and the suppression of growth of small grains. In addition, discharge voltage has a certain effect on the grain size, as is evidenced by the similarity of curves *1* and *2* in Fig. 4.

An increase in the discharge voltage leads to an increase in the energy of the sputtered atoms and, as a consequence, their mobility during adsorption on the growing coating. That is, the atoms can travel long distances and, accordingly, form larger grains. It is evident that this mechanism will be activated after a certain time from the beginning of sputtering, when the surface of the growing coating acquires a temperature sufficient to provide a slow dissipation of the energy of the adsorbed atoms.

The occurrence of kinks in curves *1* and *2* (see Fig. 4) is attributed to a jump in the rate of evacuation of the vacuum system (Fig. 4, curve *3*), which is associated with the uncontrolled leakage during deposition. If the rate of evacuation is regarded as a measure of purity of the coatings, then the samples prepared at 6 and 9 A must have the highest and lowest amount of impurities, respectively. This assumption confirms the tendency specified in [18] that the grain size increases with an increasing degree of purity of the coating.

Apparently, the grain size is determined by all three parameters—coating thickness, magnetron discharge voltage, and evacuation rate—while the ratio of con-

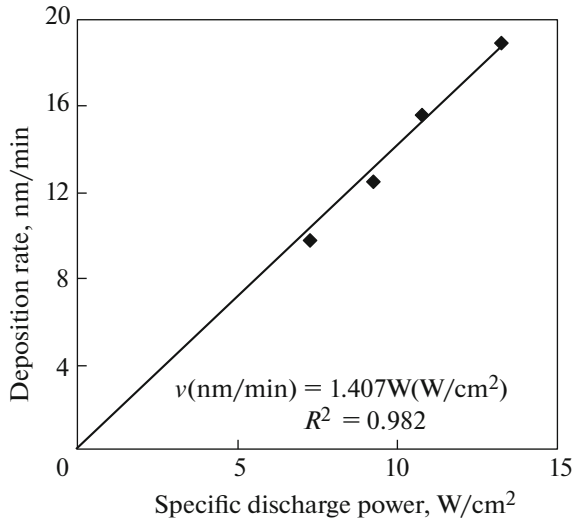

Fig. 5. Dependence of the deposition rate of AlN coatings on the magnetron discharge power density at a target–substrate distance of 70 mm, a working pressure of 0.22 Pa, and a N_2 fraction of 30 vol %.

centrations of grains with different orientations depends on the flow of impurities during nucleation.

Measurements of the AlN coating thickness showed that, with an increase in the discharge power density from 7 to 13 W/cm^2 (magnetron discharge power divided by the total area of sputtering targets), the deposition rate increases from 10 to 19 nm/min (Fig. 5).

According to expectations, the rate of deposition of AlN coatings linearly increases with an increasing magnetron discharge power density [19].

CONCLUSIONS

AlN coatings on *c*-axis oriented sapphire were prepared by dual magnetron sputtering in an Ar–N_2 gas medium with varying discharge current of sputtering of aluminum targets. According to X-ray diffraction, the coatings have a wurtzite crystalline structure and at least two types of grains with different orientations of the (002) plane. For the first type of grains, the (002) planes are nearly parallel to the substrate surface; for the second type, the planes are inclined to the substrate surface at an angle of ~14.3°. For the grains of these two types, the diameter of nuclei hardly depends on discharge current; it is 22.1 and 40.3 nm, respectively. The maximum concentration of the grains of the first type (and respective nuclei) is observed at a discharge current of 7 A; this fact is apparently attributed to the flow of impurities at the beginning of deposition.

Electron microscopy data have confirmed the occurrence of nuclei and grains of two types and shown that the grains increase in diameter with increasing discharge current and are composed of small crystallites. A larger grain size will occur in thicker coatings deposited at high discharge voltages and high rates of evacuation of the vacuum system.

Thus, the discharge current largely affects the concentration of grains with different orientations and has hardly any effect on the size of the nuclei. This feature makes it possible to control the orientation of aluminum nitride coatings; however, it does not provide the formation of an entirely single-crystal layer without modifying the magnetron sputtering method. A modification can be provided by the controlled introduction of impurities (e.g., O_2) at the initial stage of deposition to suppress the growth of grains with an undesirable orientation.

ACKNOWLEDGMENTS

The authors thank ZAO Monokristall and OOO BZS Monokristall for assistance in the research. This work was supported by the Russian Foundation for Basic Research (project no. 14-42-08047 r_ofi_m) under the state order of the Ministry of Science and Education of the Russian Federation and the strategic development program of Shukhov Belgorod State Technological University.

REFERENCES

1. Kh. Sh. Kaltaev, N. S. Sidel'nikova, S. V. Nizhankovskii, A. Ya. Dan'ko, M. A. Rom, P. V. Mateichenko, M. V. Dobrotvorskaya, and A. T. Budnikov, "Fabrication, treatment, and testing of materials and structures obtainment of textured films of aluminum nitride by thermochemical nitridation of sapphire," Semiconductors **43**, 1606 (2009).
2. A. F. Belyanen, M. I. Samoelovich, and V. D. Zhitkovsky, "Impact-resistant protective film coatings based on AlN in electronic engineering," Technol. Des. Electron. Equip. **5**, 35–41 (2005).
3. R. A. Cherkasov, S. V. Zaitsev, V. S. Vashchilin, D. S. Prokhorenkov, V. M. Narziev, and E. I. Yevtushenko, "Structural properties of thin films of AlN, grown on glass by quadrupole magnetron sputtering," in *Science and Education, Proceedings of the 6th International Research and Practice Conference, Munich, June 26–27, 2014* (Vela Verlag Waldkraiburg, Munich, 2014), pp. 452–458.
4. M. Yu. Dvoesherstov, V. I. Cherednik, A. V. Belyaev, A. V. Denisova, and A. P. Sidorin, "Heteroepitaxial Structures AlN/Al_2O_3 and GaN/Al_2O_3 for acousical electronic microwave devices," Sovrem. Naukoemk. Tekhnol., No. 9, 24–30 (2010).
5. A. F. Belyanin, M. I. Samoilovich, V. D. Zhitkovskii, and A. L. Kameneva, "Impact resistant protective film coatings based on AlN in electronics," Tekhnol. Konstrukts. Elektron. Appar., No. 5, 35–41 (2005).
6. A. F. Belyanin, V. D. Zhitkovskii, and P. V. Pashchenko, "Aluminium nitride films: production, structure and application in electron engineering devices,"

Sist. Sredstvo Svyazi, Televid. Radioveshch., No. 1, 29–37 (1998).

7. V. G. Mansurov, A. Yu. Nikitin, Yu. G. Galitsyn, S. N. Svitasheva, K. S. Zhuravlev, Z. Osvath, L. Dobos, Z. E. Horvath, and B. Pecz, "AlN growth on sapphire substrate by ammonia MBE," J. Cryst. Growth **300**, 145–150 (2007).
8. C. Ristoscu, C. Ducu, G. Socol, F. Craciunoiu, and I. N. Mihailescu, "Structural and optical characterization of AlN films grown by pulsed laser deposition," Appl. Surf. Sci. **248** (1–4), 411–415 (2005).
9. A. Claudel, E. Blanquet, D. Chaussende, R. Boichot, B. Doisneau, G. Berthomé, A. Crisci, H. Mank, C. Moisson, D. Pique, and M. Pons, "Investigation on AlN epitaxial growth and related etching phenomenon at high temperature using high temperature chemical vapor deposition process," J. Cryst. Growth **335** (1), 17–24 (2011).
10. S. Uchiyama, Y. Ishigami, M. Ohta, M. Niigaki, H. Kan, Y. Nakanishi, and T. Yamaguchi, "Growth of AlN films by magnetron sputtering," J. Cryst. Growth 189–190, 448–451 (1998).
11. D. Manova and J. W. Gerlach, and S. Mändl, "Thin film deposition using energetic ions," Materials, No. 3, 4109–4141 (2010).
12. E. I. Evtushenko, V. A. Doroganov, V. M. Nartsev, I. Yu. Moreva, S. V. Zaitsev, and S. Yu. Kolomytseva, "Modification of refractory ceramic composites with coatings based on compounds of titanium and zirconium," Refract. Ind. Ceram. **52**, 272–277 (2011).
13. V. M. Nartsev, M. S. Ageeva, D. S. Prokhorenkov, S. V. Zaitsev, S. V. Karatsupa, and V. S. Vashchilin, "Influence of deposition conditions of high-quality AlN and SiC on the coating characteristics," Vestn. Belgor. Tekhnol. Univ. V.G. Shukhova, No. 6, 168–172 (2013).
14. S. V. Zaitsev, V. S. Vashchilin, D. S. Prokhorenkov, V. M. Nartsev, and E. I. Evtushenko, "Synthesis of AlN films using vacuum-plasma technologies," Ogneupory Tekh. Keram., No. 7–8, 15–18 (2014).
15. E. V. Berlin and L. A. Seidman, *Preparation of Thin Films by Reactive Magnetron Sputtering* (Tekhnosfera, Moscow, 2014) [in Russian].
16. A. Vir Singh, S. Chandra, and G. Bose, "Deposition and characterization of c-axis oriented aluminum nitride films by radio frequency magnetron sputtering without external substrate heating," Thin Solid Films **519**, 5846–5853 (2011).
17. S. V. Zaitsev, V. S. Vashchilin, D. S. Prokhorenkov, V. M. Nartsev, and E. I. Evtushenko, "Growth and microstructure of AlN films formed by quadrupole magnetron spraying method," Ogneupory Tekh. Keram., No. 10, 13–16 (2014).
18. *Science and Technology of Thin Films,* Ed. by F. C. Matacotta and G. Ottaviani (World Scientific, Singapore, 1995).
19. K. Wasa and S. Hayakawa, *Handbook of Sputter Deposition Technology. Principles, Technology and Application* (Noyes Publ., Westwood, 1992).

Translated by M. Timoshinina